

Supplementary Information

Sc₃N@C₈₀ and La@C₈₂ Doped Graphene for a New Class of Optoelectronic Devices

Kishan Jayanand¹⁺, Srishti Chugh^{1,2+}, Nirmal Adhikari³, Misook Min¹, Luis Echegoyen^{4}, and Anupama B. Kaul^{1,5*}*

¹Department of Materials Science and Engineering, PACCAR Technology Institute, University of North Texas, Denton, TX 76203, U.S.A.

²Department of Metallurgical, Materials and Biomedical Engineering, University of Texas at El Paso, El Paso, TX 79968, U.S.A.

³Department of Electrical Engineering, ⁴Department of Chemistry, University of Texas at El Paso, El Paso, TX 79968, U.S.A.

⁵Department of Electrical Engineering, University of North Texas, Denton, TX 76203, U.S.A.

⁺These authors contributed equally to the work

^{*}Corresponding Author Email: anupama.kaul@unt.edu; echegoyen@utep.edu

Electrophoretic Deposition of END₁

Dispersions of END₁ (~ 0.01 mg, ~ 0.5 mg, and ~ 1 mg) exhibited optical absorption spectra in ~ 1 mL of o-DCB shown in Figure S1(a). Since endohedral fullerenes have low solubility in toluene, o-DCB was used for the dissolution of END₁.^[1] END₁ suspensions shows a relatively high absorbance for $\lambda \sim 450\text{-}680\text{ nm}$, consistent with previous reports.^[2] As the concentration of END₁ in o-DCB was increased, the absorption of END₁ also increased, consistent with the Lambert-Beer Law. Electrophoretic deposition was used to adhere END₁ on the substrate, similar to the technique reported for depositing C₆₀ films,^[3] where the current I as a function of the electrophoretic deposition time t is shown in Figure S1(b). A drop of the suspension was injected at voltage $V \sim 0\text{ V}$ and a step potential was applied from ~ 0.05 V to ~ 0.3 V in ~ 0.05 V increments between the electrodes. The electrophoretic deposition I increased gradually as the step-potential increased with time for END₁. Upon saturation for a particular step V , I starts to decrease due to Joule heating as the resistance increases. After $t \sim 12\text{ min}$ of deposition, a film of END₁ adhered on top of the Au/Ti electrodes. Eventually, the device was vacuum annealed for ~ 24 hours at ~ 180°C to drive off the residual solvents (i.e. at the approximate

boiling temperature of o-DCB). Prior to the fabrication of the END₁-graphene hybrid devices, reference measurements were conducted for END₁ in ~1 mL of o-DCB to gauge the optimal concentration needed of the END₁ in the construction of the graphene hybrid devices.

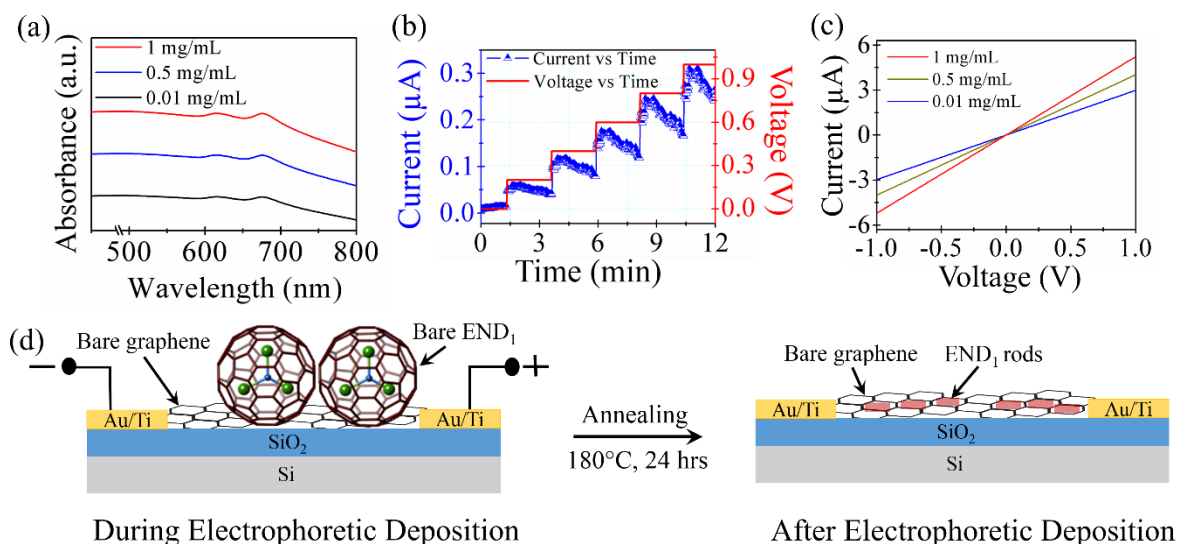


Figure S1: (a) Optical absorbance at various concentrations of END₁ as a function of λ . (b) Current measurements as a function of electrophoretic deposition time. (c) I - V of END₁ at various concentrations in o-DCB. (d) Schematic illustration for the electrophoretic deposition of END₁ on the graphene membrane. The graphene was mechanically exfoliated and Au/Ti electrical contacts were deposited followed by a lift-off process using SiO₂/Si substrate (schematic not to scale). For electrophoretic deposition, a ~ 1 mg suspension solution of END₁ in ~ 1 mL of o-DCB was used. During electrophoretic deposition, individual atoms of END₁ aggregated on top of the graphene membrane, but after annealing the hybrid for ~ 24 hrs at ~ 180 °C, END₁ aligns itself in the form of a rod-shaped crystal as shown schematically in the right image of (d).

The I - V Characteristic of bare END₁ films deposited on SiO₂/Si substrates for concentrations ~ 0.01 mg/mL, ~ 0.5 mg/mL and ~ 1 mg/mL under vacuum conditions are shown in Figure S1(c) from ~ -1 V to ~ 1 V. Since the ~ 1 mg/mL concentration of END₁ yielded the highest I values in o-DCB, this concentration was used to electrophoretically deposit the END₁ on top of the graphene membrane. Figure S1(d) shows a schematic depiction of the hybrid structure of END₁ aggregated on top of the graphene membrane, where the

aggregated film consists of individual END₁ molecules. However, after annealing the hybrid devices, END₁ aligns itself in the form of a rod-shaped crystal, as shown in Figure S1(d)-right. The END₁ molecules nucleate rapidly and then the crystal seeds start to grow via π - π stacking to form small particles where the growth of END₁ occurs along the long-axis and the crystals adopt a rod-shaped morphology,^[2] as confirmed using SEM.

SEM and AFM Imaging Analysis END₁

SEM measurements were conducted to see the agglomeration of END₁ on top of graphene membrane. Figures S2(a)-(d) show typical SEM images of END₁ ((a) and (c)) and END₁-graphene ((b) and (d)), where the top-left inset of Figure S2(b) shows the bare graphene device only. The average length of END₁ rod-shaped ensembles after electrophoretic deposition was found to be $\sim 4 \mu\text{m}$ as shown in Figure S2(c) and (d). More insights into the structural morphology was obtained using AFM conducted at a scan speed of 1 Hz. The height profile measurements were performed over an area of $\sim 15 \mu\text{m} \times 15 \mu\text{m}$, as shown in Figure S2(e)-(i). The height profile from Figure S2(e)-(i) (red dotted lines) is reproduced in Figure S2(e)-(ii) which reveals the relatively smooth surface of the bare graphene membrane, where the inset shows the height profile of bare graphene with 24 nm thickness. Similar AFM measurements were performed for bare END₁ and END₁-graphene hybrid structures, as shown in Figures S2(f) and (g), respectively. Figures S2(f)(i)-(ii) illustrate the clusters of bare END₁ in the form of islands exhibiting a peak height of $\sim 3.6 \text{ nm}$ and diameter $\sim 50 \text{ nm}$; Figures S2(g)(i)-(ii) on the other hand, show clustering of END₁ on the graphene surface with a peak height of $\sim 9\text{-}20 \text{ nm}$ and cluster diameter $\sim 200\text{-}350 \text{ nm}$.

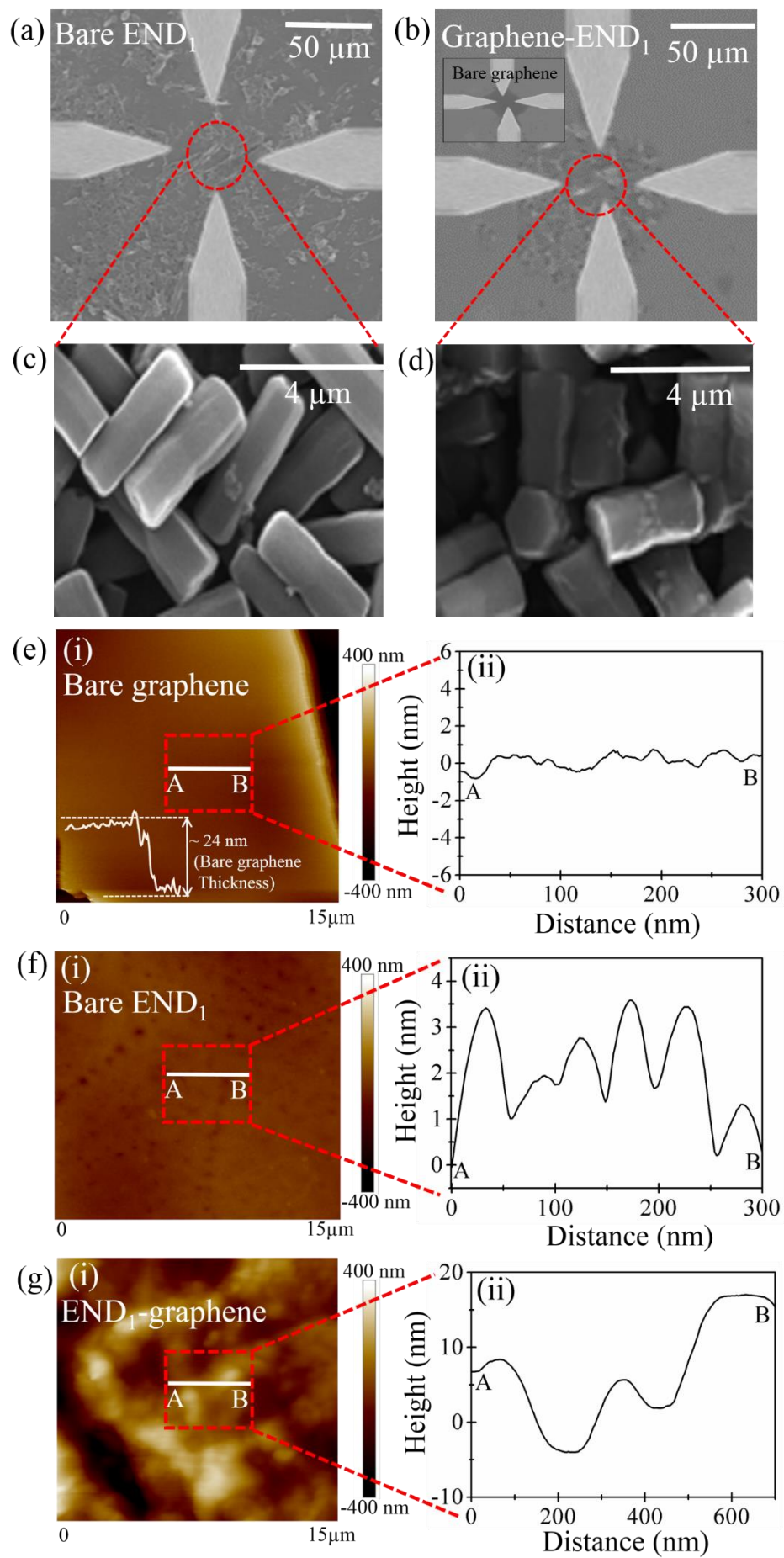


Figure S2: Low-magnification SEM images of electrophoretic deposition of (a) bare END₁, (b) END₁-graphene hybrid (inset shows the SEM of bare graphene). High-magnification SEM images showing (c) the micron-sized hexagonal END₁ rods with an average length of $\sim 4 \mu\text{m}$, and (d) the aggregation of END₁ on top of the graphene membrane after electrophoretic deposition. (e)-(g): (i) Large-area AFM scan ($\sim 15 \mu\text{m} \times 15 \mu\text{m}$), and (ii) shows the height profile of the A-to-B scan direction. The image in (e)-(i) reveals a uniform, smooth graphene surface, where the bottom left inset shows the bare graphene thickness to be $\sim 24 \text{ nm}$ thickness. (f)-(i)-(ii) illustrate the clusters of bare END₁ in the form of islands with a peak height of $\sim 3.6 \text{ nm}$ and diameter of $\sim 50 \text{ nm}$; (g)-(i)-(ii) reveal the clustering of END₁ on the graphene surface in the form of islands with peak height of $\sim 9\text{-}20 \text{ nm}$ and diameter of $\sim 200\text{-}350 \text{ nm}$.

Electrophoretic Deposition of END₂

Before the preparation of the END₂-graphene hybrid devices, initial measurements were conducted on the bare END₂ to measure the intrinsic conductance of these endohedrals, where ~ 0.1 , ~ 0.2 , and $\sim 0.3 \text{ mg}$ of END₂ was dissolved in $\sim 1 \text{ mL}$ of o-DCB. Electrophoretic deposition was used to adhere END₂ on the substrate, similar to the technique reported for depositing C₆₀ films,^[3] where the current I as a function of the electrophoretic deposition time t is shown in Figure S3(a). A drop of the suspension was injected at voltage $V \sim 0 \text{ V}$ and a step potential was applied from $\sim 0.05 \text{ V}$ to $\sim 0.3 \text{ V}$ in $\sim 0.05 \text{ V}$ increments between the electrodes.

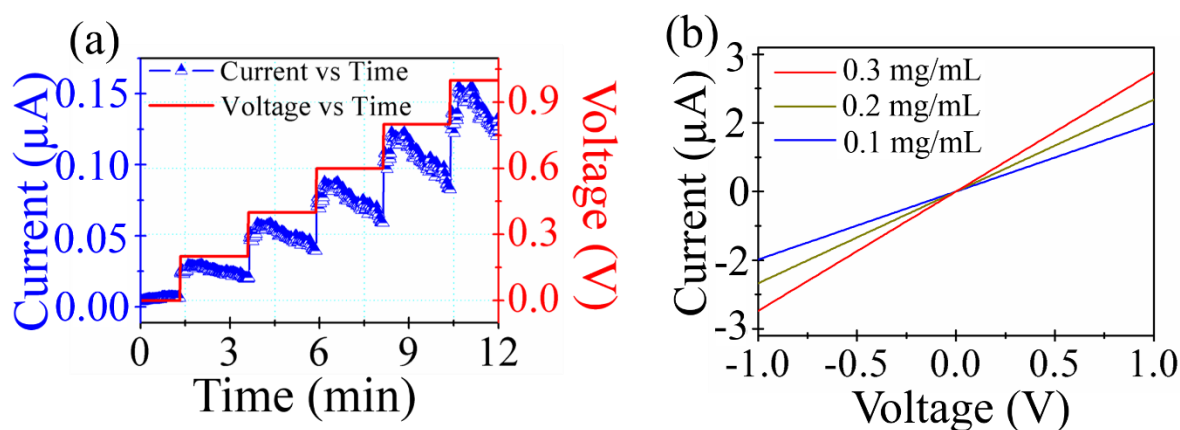


Figure S3: (a) Current measurements as a function of electrophoretic deposition time for END₂. (b) I - V Characteristic of END₂ at various concentrations in o-DCB.

The electrophoretic deposition I increased gradually as the step-potential increased with time for END₂. Upon saturation for a particular step V , I starts to decrease due to Joule heating as the resistance increases. After $t \sim 12$ min of deposition, a film of END₁ adhered on top of the Au/Ti electrodes. Eventually, the device was vacuum annealed for ~ 24 hours at $\sim 180^\circ\text{C}$ to drive off the residual solvents (i.e. at the approximate boiling temperature of o-DCB). The I - V Characteristic of bare END₂ films deposited on SiO₂/Si substrates for concentrations ~ 0.1 mg/mL, ~ 0.2 mg/mL and ~ 0.3 mg/mL under vacuum conditions are shown in Figure S3(b) from ~ -1 V to ~ 1 V. Since the ~ 0.3 mg/mL concentration of END₂ yielded the highest I values in o-DCB, this concentration was used to electrophoretically deposit the END₂ on top of the graphene membrane.

AFM Imaging of END₂

Figures S4(a) and (b) show the representative AFM images of the bare END₂ and END₂-graphene hybrid at a scan speed of ~ 1 Hz. The height profile of the region with the END₂ clusters was performed using AFM analysis, where the $\sim 15\ \mu\text{m} \times 15\ \mu\text{m}$ scan area is shown in Figure S4(a)-(i), over the A to B scan direction as illustrated in Figure S4(a)-(ii), where the bare graphene AFM scan profile height was ~ 12.8 nm. Figure S4(a)(i)-(ii) illustrate the clusters of bare END₂ in the form of islands exhibiting a height of ~ 35 - 40 nm and diameter ~ 170 - 250 nm; the cluster arrangement for END₂ on graphene is seen in Figure S4(b)(i)-(ii), which reveals a height ~ 45 - 55 nm and diameter ~ 184 - 240 nm for the clusters.

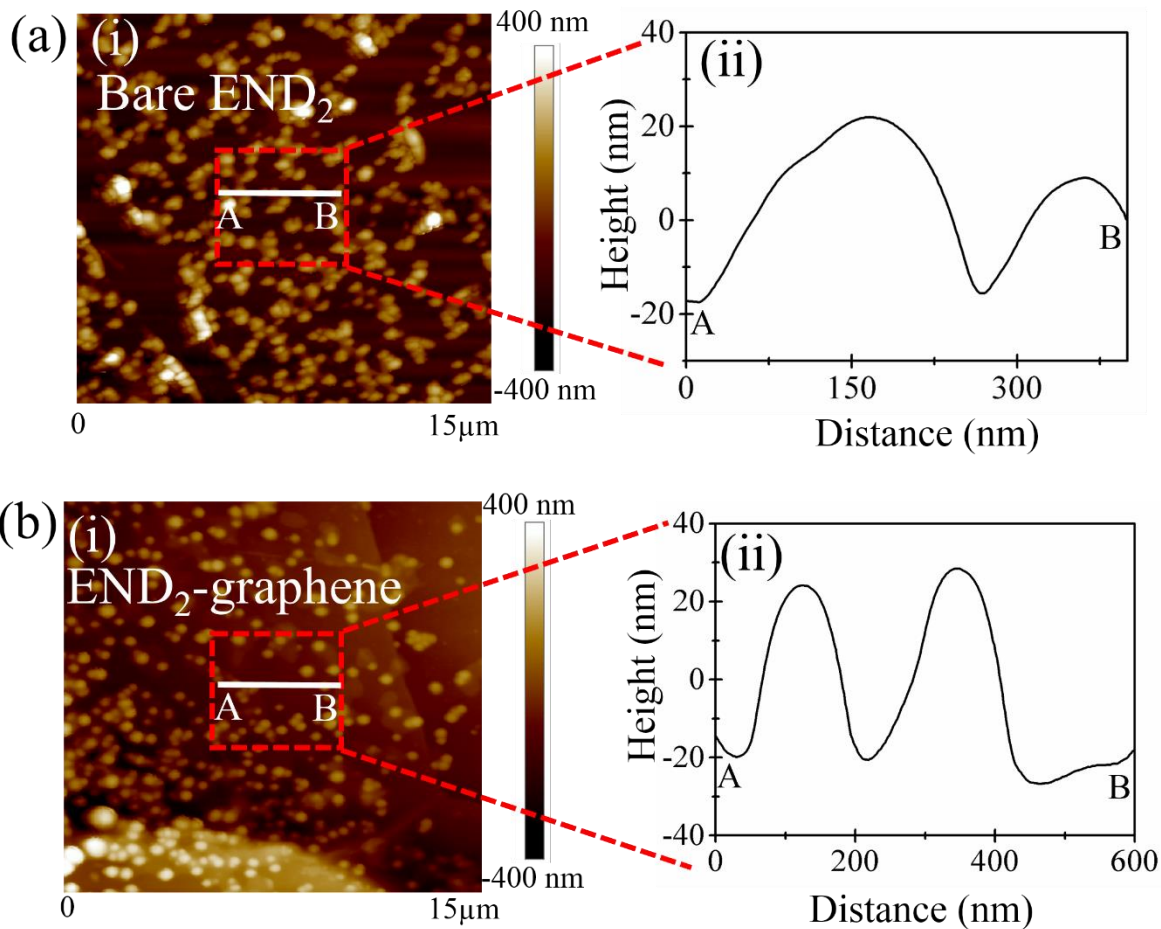


Figure S4: (a) and (b): (i) Large-area ($\sim 15\ \mu\text{m} \times 15\ \mu\text{m}$) AFM scan and (ii) illustrates the clusters of bare END_2 in the form of islands with a height of $\sim 35\text{-}40\ \text{nm}$ and diameter $\sim 170\text{-}250\ \text{nm}$ in the A-to-B scan direction; (b)(i)-(ii) reveals the clustering of END_2 on the graphene surface in the form of islands $\sim 45\text{-}55\ \text{nm}$ and diameter $\sim 184\text{-}240\ \text{nm}$ in diameter. The height of the bare graphene was measured to be $\sim 12.8\ \text{nm}$ using AFM.

REFERENCES

- [1] M. N. Chaur, F. Melin, A. L. Ortiz, L. Echegoyen, *Angew. Chemie - Int. Ed.* **2009**, 48, 7514.
- [2] Y. Xu, J. Guo, T. Wei, X. Chen, Q. Yang, S. Yang, *Nanoscale* **2013**, 5, 1993.
- [3] P. V Kamat, S. Barazzouk, K. G. Thomas, S. Hotchandani, *J. Phys. Chem. B* **2000**, 104, 4014.